Diluted neural network with refractory periods

Crisógono R. da Silva,[1,*] Francisco A. Tamarit,[2,†] and Evaldo M. F. Curado[1,‡]
[1]*Centro Brasileiro de Pesquisas Físicas, Rua Xavier Sigaud 150, 22290-180 Rio de Janeiro, Brazil*
[2]*Fa.M.A.F., Universidad Nacional de Córdoba, Ciudad Universitaria, 5000 Córdoba, Argentina*
(Received 16 September 1996)

We study an extreme and asymmetrically diluted version of the Hopfield model when the refractory period is taken into account in the dynamics of the neurons through a time dependent threshold. We present an analytical approach that allows one to preserve, in an approximate way, the dependence of the system on its whole history. In particular, we obtain a recurrent equation for the overlap from which one can analyze the retrieval capacity. We also perform numerical simulations that are well fitted by our analytical results. Depending on the amplitude of the potential that mimics the effect of the refractory period and on the ratio α between the number of stored patterns p and the mean connectivity per neuron C, the system presents different dynamical behaviors and retrieval abilities. [S1063-651X(97)15603-3]

PACS number(s): 87.10.+e, 84.35.+i, 64.60.Ht

I. INTRODUCTION

In the past decade a huge effort has been devoted to the study of the Hopfield model for associative memory [1]. It basically consists of a *fully connected* network of *binary units* evolving according to a threshold dynamics and coupled through a *symmetric* synaptic matrix. Both the symmetry of the couplings and the full connectivity make the model mathematically tractable, and its analogy with Ising spin glasses models is straightforward. One can also introduce a noise parameter T that mimics the randomness involved in the biological process [2], and treat it as a generalized temperature introduced through a stochastic Monte Carlo dynamics. Now the long-time behavior of the model can be easily obtained from a thermodynamical analysis that follows that usually applied to mean-field Ising spin glass models. Recently, Coolen and Sherrington [3] have developed a procedure that reproduces the correct dynanical equations of the fully connected Hopfield model (near saturation) for short times and in equilibrium. For intermediate time scales, it does not lead to the exact equations, but succeeds in capturing the main characteristics of the flows in the order parameter plane [4].

However, biological neural networks have a high degree of asymmetry in its synapses and are sparsely interconnected. This means that those two elements that make the Hopfield model mathematically tractable, namely, *full connectivity* and *symmetry*, simultaneously limit seriously its ability for modeling real systems. In order to improve the model from a biological point of view, different modifications have been introduced in the literature. Most of them preserve the Hebbian prescription for the synaptic matrix, and add biological ingredients like dilution and asymmetry, among others [5–9]. The main mathematical consequence of removing symmetry in the synapses is to eliminate a statistical mechanics approach. One is then restricted to studying only the dynamics of the system, which is hard to treat analytically. A simple way of introducing both dilution and asymmetry is to cut the synapses J_{ij} and J_{ji} with probability $(1-C/N)$ independently of each other, where C is the mean connectivity of each neuron and N the number of neurons in the network. In particular, in the strong dilution limit $C \ll \ln N$, Derrida, Gardner, and Zippelius [10] solved exactly the dynamics of the systems. Further, Arenzon and Lemke [11] have shown through numerical simulation that this analytical approach is also valid for the less strong condition $C \ll N$.

On the other hand, it is also well known that after firing a spike, a neuron is unable to fire again, for a period of time of the order of 2 ms and irrespective of its afferent potential. This short period is known as the *absolute refractory period* (ARP). Following this ARP and during about 4 ms the neuron can fire again but now with a greater potential threshold which decreases with time. This second interval is known as the *relative refractory period*. In the last year, a lot of work has been devoted to studying different ways of including this biological feature in several neural models, but most of them treat fully connected versions which are very unplausible [12–19]. The simplest way of modeling this behavior is to introduce a time dependent threshold that acts only on those neurons that have emitted a signal and favors them to be at rest during a given time interval.

In the present work we introduce a time dependent threshold that mimics the refractory periods in an extremely diluted Hopfield model. We will see that, unlike the usual extremely diluted version, one cannot now neglect temporal correlations. In this sense one can say that this work is not a mere extension of calculation introduced in [10], but includes a

*Electronic address: crsilva@cbpfsu1.cat.cbpf.br. Also at Departamento de Física, Universidade Federal de Alagoas, Cidade Universitária, BR 101 Km 14 Norte, 57072-340 Maceió, Brazil.
†Electronic address: tamarit@fis.uncor.edu
‡Also at International Centre of Condensed Matter Physics (C.P. 04667, 70919-970 Brasilia, Brazil) and Department of Physics, Universidade de Brasilia, Brasilia, Brazil. Electronic address: curado@iccmp.br

different mathematical approach. We obtain a recurrent equation for the overlap between the state of the system and the memories that take into account, in an approximate form, *the whole history of the network*. We also show that our analytical results, although not exact, fit very well with those observed in numerical simulations. This paper is organized as follows. In Sec. II we introduce the model. In Sec. III we describe our analytical approach and present the results. In Sec. IV we compare the analytical results with those obtained through numerical simulations. Finally, in Sec. V we discuss the main results.

II. MODEL

Let us consider a network of N binary neurons, each one modeled by an Ising-like variable S_i $(i=1,N)$, which can take the values $\{-1,+1\}$ representing the passive and active states, respectively. The time evolution of the network at time $t+1$ is governed by a synchronous stochastic dynamics ruled by the following probability:

$$\mathrm{Prob}(S_i(t+1))=\tfrac{1}{2}(1+S_i(t+1)\tanh\beta_0 h_i(t)), \tag{1}$$

where $\beta_0=1/T_0$ measures the noise level of the network and $h_i(t)$ denotes the post-synaptic potential (PSP) of the ith neuron at time t

$$h_i(t)=h_i^H(t)-\frac{\Delta_0}{2}(S_i(t)+1). \tag{2}$$

Here h_i^H denotes the usual Hopfield PSP with asymmetric dilution,

$$h_i^H=\sum_{j\neq i}^{N} C_{ij}J_{ij}S_j(t), \tag{3}$$

and the synaptic matrix J_{ij} is defined by the Hebbian rule

$$J_{ij}=\sum_{\mu=1}^{p}\xi_i^\mu\xi_j^\mu. \tag{4}$$

The ξ_i^μ's are quenched random independent variables taking the values ±1 with equal probability. Hence ξ_i^μ denotes the state of the ith neuron in the μth stored pattern $(\mu=1,\ldots,p)$. C_{ij}'s introduce the asymmetric dilution of the synapses, and are random variables chosen according to the following distribution:

$$\rho(C_{ij})=\frac{C}{N}\delta(C_{ij}-1)+\left(1-\frac{C}{N}\right)\delta(C_{ij}). \tag{5}$$

Then C is the mean connectivity per neuron. The second term in Eq. (2) is included to mimic the refractory period. If neuron i emits a spike at time t $(S_i(t)=+1)$, then an extra contribution to the PSP $-\Delta_0$ acts like a time dependent threshold which favors the neuron to be at rest at $t+1$. If, on the other hand, neuron i is inactive $(S_i(t)=-1)$, then it works like an usual Hopfield neuron. It is important here to stress that this model does not distinguish between absolute and relative periods. Instead, it considers a kind of average to determine the refractory periods: large Δ_0 means that Δt is about of 2 ms, while small Δ_0 means that Δt is about 4 or 5 ms.

Due to the lack of detailed balance in the dynamics of our model, it is not possible to use a thermodynamical approach. Thus, in this paper we will restrict ourselves to consider the long-time dynamical behavior of the system by looking for a recurrent equation for the macroscopic overlap between the state of the system and the memories, defined as

$$m^\mu(t)=\frac{1}{N}\sum_{i=1}^{N}\xi_i^\mu\langle S_i(t)\rangle. \tag{6}$$

Here $\langle\,\rangle$ denotes both an average over the initial conditions and a thermal one.

It is important to note that in our model the violation of the detailed balance condition is not only due to the asymmetry of the synapses, but also to the inclusion of the time dependent threshold. In the absence of this term, the so called *strong dilution* condition $C\ll\ln N$ allows one to obtain an exact recurrent equation for m^μ by replacing the quenched average by an annealed one [10]. However, when the refractory period is included as a threshold that depends on the state of the same neuron, this approach is not longer valid. Thus we are forced to take into account the whole history of the network. Since an exact analytical treatment along these lines is too hard to be implemented in our model, in Sec. III we introduce and develop an approximate method from which we study its recognition ability. The validity of our approach is tested in Sec. V, where we performed a numerical study of the system.

III. DYNAMICAL EQUATION

We start by assuming that the initial configuration $\{S_i(0)\}$ has a macroscopic overlap only with the first memory $[m^1(0)=m$ and $m^\mu(0)\sim O(N^{-1/2})$ for $\mu>1]$, and that the system will never jump to another memory attractor. That is, the other $p-1$ overlap will be always macroscopically zero. This last assumption is justified by our numerical results, as described in Sec. V. From definition (1), and after taking the thermodynamical limit $N\to\infty$, $m^1(t+1)\equiv m(t+1)$ can be rewritten as

$$\begin{aligned} m(t+1)&=\frac{1}{N}\sum_{i=1}^{N}\xi_i^1\tanh\beta_0\left(h_i^H(t)-\frac{\Delta_0}{2}(S_i(t)+1)\right)\\ &=\left\langle\left\langle\xi_i^1\tanh\beta_0\left(h_i^H(t)-\frac{\Delta_0}{2}(S_i(t)+1)\right)\right\rangle\right\rangle, \end{aligned} \tag{7}$$

where $\langle\langle\,\rangle\rangle$ denotes a configurational average over the quenched random variables $\{\xi_i^\mu\}$. Note that although we have already made the thermal average, in Eq. (7) we maintain the explicit dependence on $S_i(t)$ of the refractory term. In a mean-field approach one would replace it by $\xi_i^1 m(t)$. We have in fact performed this calculation, but the results obtained showed to be far from describing the numerical ones. Instead we preserve such dependence on the history of the system by averaging again $S_i(t)$ according to Eq. (1). In doing so, we now also include a dependence on $t-1$. The same procedure can now be repeated until we finally attain

the initial state $S_i(0)$. It can be easily verified that this mechanism yields to the following expression:

$$m(t+1)=\tfrac{1}{2}\langle\langle \xi_i^1 A_i(t)\rangle\rangle+\frac{1}{2^2}\langle\langle \xi_i^1 B_i(t)A_i(t-1)\rangle\rangle + \frac{1}{2^3}\langle\langle \xi_i^1 B_i(t)B_i(t-1)A_i(t-2)\rangle\rangle+\cdots + \frac{1}{2^{t+1}}\langle\langle \xi_i^1 B_i(t)B_i(t-1)\ldots B_i(1)A_i(0)\rangle\rangle = \left\langle\left\langle \xi_i^1 \sum_{l=0}^{t}\frac{1}{2^{l+1}}A_i(t-l)\prod_{q=1}^{l}B_i(t-(q-1))\right\rangle\right\rangle, \tag{8}$$

where $A_i(t)$ and $B_i(t)$ are given by

$$A_i(t)=\tanh[\beta_0(h_i^H(t)-\Delta_0)]+\tanh[\beta_0 h_i^H(t)],$$

$$B_i(t)=\tanh[\beta_0(h_i^H(t)-\Delta_0)]-\tanh[\beta_0 h_i^H(t)]. \tag{9}$$

Next we assume that the temporal correlations among states of the system at different times can be neglected, i.e., all factors at different times in each term in Eq. (8) can be independently averaged:

$$\left\langle\left\langle A_i(t-l)\prod_{q=1}^{l}B_i(t-(q-1))\right\rangle\right\rangle = \langle\langle A_i(t-l)\rangle\rangle\prod_{q=1}^{l}\langle\langle B_i(t-(q-1))\rangle\rangle. \tag{10}$$

This assumption, together with the strong dilution condition, makes our problem mathematically tractable. Under these conditions, $h_i(t)$ can be considered as a random variable which, in the limit $C\to\infty$, $p\to\infty$ with $\alpha\equiv p/C$ constant, has a Gaussian distribution whose mean value and variance are m and α, respectively. After some standard calculations, we then obtain the following approximation for the recurrent equation:

$$m(t+1)=\sum_{l=0}^{t}\frac{1}{2^{l+2}}\left[A_-(t-l)\prod_{q=1}^{l}B_-(t-(q-1)) + (-1)^l A_+(t-l)\prod_{q=1}^{l}B_+(t-(q-1))\right], \tag{11}$$

with

$$A_\pm(t)=\int Dz[\tanh(\beta(m(t)+z\sqrt{\alpha}\pm\Delta)) + \tanh(\beta(m(t)+z\sqrt{\alpha}))],$$

$$B_\pm(t)=\int Dz[\tanh(\beta(m(t)+z\sqrt{\alpha}\pm\Delta)) - \tanh(\beta(m(t)+z\sqrt{\alpha}))]. \tag{12}$$

Here $\beta=1/T=C/T_0$ and $\Delta=\Delta_0/C$ define the reduced temperature and the reduced refractory parameter, respectively, and Dz is given by

$$Dz=\frac{dz}{\sqrt{2\pi}}e^{-z^2/2}.$$

Note that for $\Delta=0$, $B_\pm(t)=0$ for all t and only the term $l=0$ survives in Eq. (11). So we recover the expression obtained by Derrida, Gardner, and Zippelius in [10].

In spite of our approximations, Eq. (11) still depends on the whole history of the neuron. A first simplification consists in truncating the series to a given finite order, that is, taking into account only the l previous states of the network. In doing so, we first observe that it always yields to a fixed point attractor, independently of the order of the truncation. Finally, we also verify that for small values of Δ a truncation to order 4 seems to be enough to fit the numerical results while for large Δ all the terms are necessary. In what follows we assume that the system always evolves to a fixed point, and that the corresponding equation takes the form

$$m=\frac{1}{4}\sum_{l=0}^{\infty}\frac{1}{2^l}[A_-B_-^l+(-1)^l A_+B_+^l]. \tag{13}$$

Here $A_\pm$ and $B_\pm$ are given by Eq. (12) with $m(t)=m$ for all t. In Sec. V we will show through the numerical results that this assumption is valid for a wide range of values of Δ. Fortunately, it can be easily verified that in the limit $l\to\infty$ this series converges to the following expression:

$$m=\frac{1}{2}\sum_{\sigma=\pm}\frac{\int Dz[\tanh(\beta(m+z\sqrt{\alpha}-\sigma\Delta))+\tanh(\beta(m+z\sqrt{\alpha}))]}{2-\sigma\int Dz[\tanh(\beta(m+z\sqrt{\alpha}-\sigma\Delta))-\tanh(\beta(m+z\sqrt{\alpha}))]}. \tag{14}$$

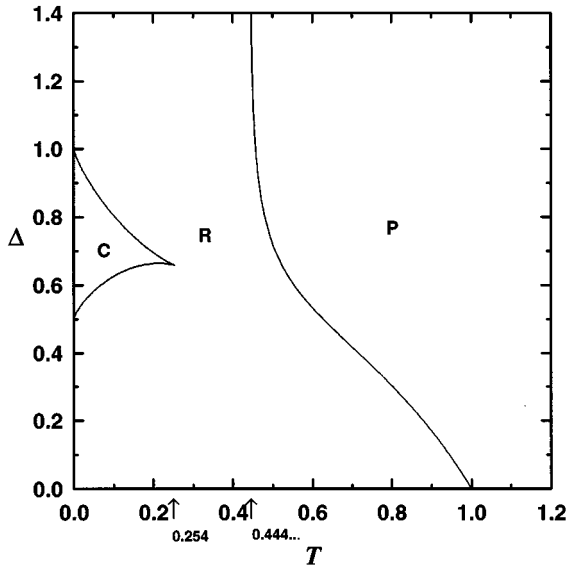

FIG. 1. Phase diagram Δ vs T for $\alpha=0$.

A. Finite number of memories

Next we consider the $\alpha=0$ case, for which Eq. (14) take the simple form

$$m=\frac{1}{2}\sum_{\sigma=\pm}\frac{\tanh(\beta(m-\sigma\Delta))+\tanh(\beta m)}{2-\sigma[\tanh(\beta(m-\sigma\Delta))-\tanh(\beta m)]}. \quad (15)$$

Figure 1 displays the phase diagram Δ vs T. For any value of Δ the system suffers a second order phase transition from a recognition phase (R) characterized by a $m\neq 0$ attractor to a paramagnetic phase (P) characterized by the $m=0$ solution. Since the transition is continuous, we expand Eq. (15) for small values of m, and obtain the following expression for the critical line:

$$T_c=\frac{4+2\tanh(\beta_c\Delta)-2\tanh^2(\beta_c\Delta)}{(2+\tanh(\beta_c\Delta))^2}. \quad (16)$$

As $\Delta\to 0$, we then obtain the well known standard Hopfield case with $T_c=1$. On the other hand, for $\Delta\to\infty$ we obtain $T^*=4/9=0.444\ldots$. In the recognition phase we observe three different behaviors. For small values of Δ the retrieval is almost perfect ($m\approx 1$). For large values of Δ the recognition ability is very poor, even at $T=0$, with $m\leqslant 0.5$. Finally, in the intermediate region ($0.5<\Delta<1$) the retrieval regime depends on the temperature: for $T<0.254$ we found a small region (C) where these two different retrieval solutions coexist, one close to 1 and the other close to 0.5. The system chooses one or the other depending on the initial value of the overlap. For $T>0.254$ the system goes continuously from the high recognition regime to the poor one as Δ increases.

In Fig. 2 we present the behavior of the overlap m as a function of Δ for different values of T. For $T=0$ and 0.1, we observe the three different regimes described in Fig. 1. For small Δ the system has only one stable solution $m\approx 1$; that is, for any macroscopic initial overlap with the memory the system almost perfectly recognizes the pattern. As Δ increases the system suffers a first order dynamical transition where a retrieval attractor emerges with $m\approx 0.5$. The dashed

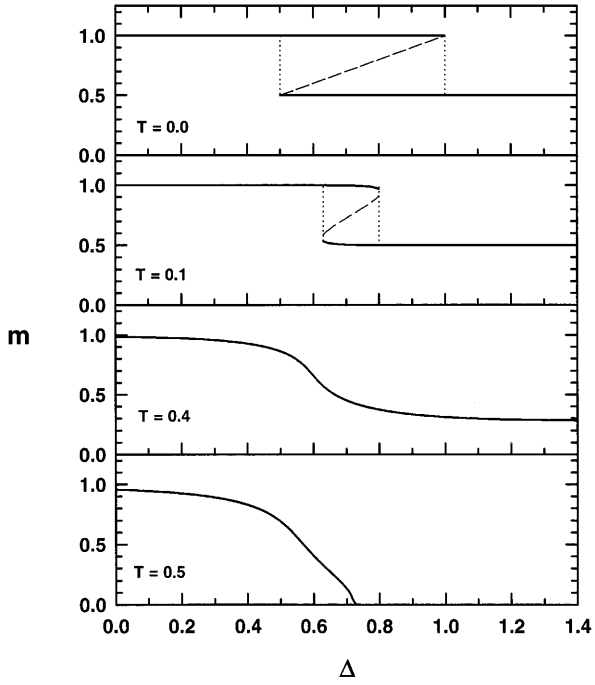

FIG. 2. The final overlap m as a function of Δ for $\alpha=0$ and for different values of T (0, 0.1, 0.4, and 0.5).

lines indicate the unstable solutions that separates the basins of attraction of the two coexisting stable solutions. Finally, for large Δ the system undergoes a dynamical phase transition where the solution with high overlap discontinuously disappears. In this phase the system can only poorly recognize the memory for any finite initial overlap. For $T=0.4$ the system always recognizes the pattern, but its performance decreases asymptotically to a finite value as Δ increases. The same behavior is observed in the interval $0.254<T<0.444\ldots$. Finally, for $T=0.5$ we see that the system suffers a second order dynamical transition from the retrieval phase to the paramagnetic phase, and this behavior is qualitatively the same for any temperature such that $0.444<T<1$ (see Fig. 1).

B. Infinite number of memories

In this section we consider the $\alpha\neq 0$ case. Let us start analyzing the noiseless case $T=0$ for which we have performed numerical simulations. After same simple calculations, Eq. (14) takes the following form:

$$m=\frac{1}{2}\sum_{\sigma=\pm}\frac{\mathrm{erf}\left(\frac{m-\sigma\Delta}{\sqrt{2\alpha}}\right)+\mathrm{erf}\left(\frac{m}{\sqrt{2\alpha}}\right)}{2-\sigma\left[\mathrm{erf}\left(\frac{m-\sigma\Delta}{\sqrt{2\alpha}}\right)-\mathrm{erf}\left(\frac{m}{\sqrt{2\alpha}}\right)\right]}. \quad (17)$$

In Fig. 3 we present the phase diagram Δ vs α. Note that in this case the parameter α plays a similar role to the temperature in the $\alpha=0$ limit. The second order transition lines are displayed for the truncated series to orders $l=4$, 6, and 8 and when the whole series is taken into account ($l=\infty$). Note that, as we previously stressed, for small Δ it is enough to

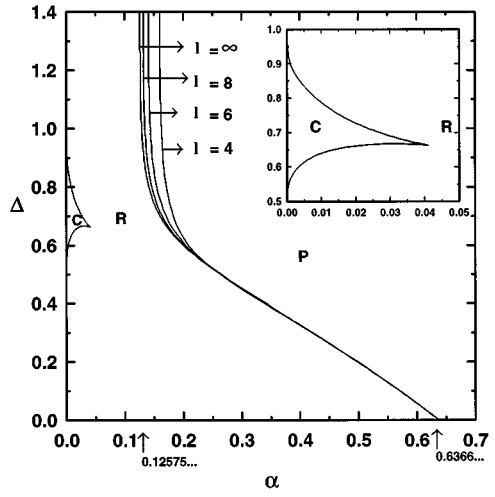

FIG. 3. Phase diagram Δ vs α at $T=0$. The critical line separating the paramagnetic and retrieval phase is showed for $l=4$, 6, 8, and ∞.

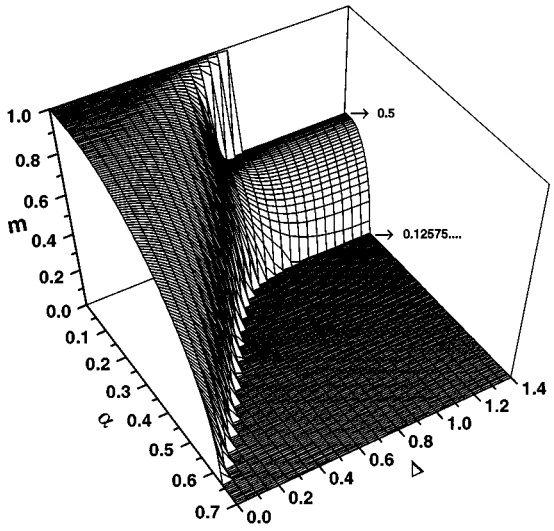

FIG. 4. The overlap as a function of α and Δ at $T=0$ with initial overlap $m_0=1$.

truncate the series to order 4, but for large Δ one has to sum over all the terms. Expanding the former equation for small values of m, we obtain the following relation between the parameters Δ and α at the critical line:

$$\alpha_c=\frac{8}{\pi}\left[\frac{1+\ \mathrm{erf}\left(\frac{\Delta}{\sqrt{2\alpha_c}}\right)+e^{-\Delta^2/2\alpha_c}}{\left[2+\ \mathrm{erf}\left(\frac{\Delta}{\sqrt{2\alpha_c}}\right)\right]^2}\right]^2. \tag{18}$$

For $\Delta=0$ we recover the maximum stored capacity $\alpha_c=2/\pi$ obtained in [10]. In the opposite limit $\Delta\to\infty$, the transition line tends asymptotically to $\alpha^*=32/81\pi\approx 0.125$.

In Fig. 4 we plot m as a function of α and Δ when the initial configuration is close to the related pattern ($m_0\approx 1$). For $\Delta=0$ we recover the transition line obtained in [10,11]. For large Δ and small α this equation predicts that the system retrieves the pattern with a low value of the overlap. Actually, as will be discussed in Sec. IV, in this region the systems recognizes through a cycle 2 orbit. Thus our initial assumption concerning the existence of a fixed point attractor fails. Nevertheless, in this cyclic orbit the parameter m fluctuates around a value that agrees very well with that obtained from the fixed point equation.

Finally, we also consider the $T\neq 0$ case. Expanding Eq. (14) for small m, we obtain after some calculations the equation for the critical surface in the space (T,α,Δ),

$$T_c=2\left[\frac{2+\int Dz(f_+-f_0)-\int Dz f_0^2\left(1+\int Dz f_+\right)-\int Dz f_+^2\left(1-\int Dz f_0\right)}{\left[2+\int Dz(f_+-f_0)\right]^2}\right], \tag{19}$$

where f_+ and f_0 are given by

$$f_+=\tanh\left(\frac{\sqrt{\alpha}z+\Delta}{T_c}\right),\quad f_0=\tanh\left(\frac{\sqrt{\alpha}z}{T_c}\right).$$

In Fig. 5 we show the phase diagram in the T, α, and Δ space. For $\Delta=0$ and large α the critical line approaches the $T=0$ axis continuously at $\alpha_c=2/\pi$ [10]. Along the critical surface the system undergoes a continuous transition from the retrieval phase (below) to the paramagnetic phase (above). Note that below this critical surface there exists a small volume where two different recognition solutions coexist, but is not shown in this diagram.

IV. NUMERICAL SIMULATIONS

In order to test the results of the analytic approach presented in this paper, we also performed numerical simulations of our model in the noiseless limit. Actually, the extreme dilution condition $C\ll\ln N$ is hard to implement in any computer but, as stressed in Sec. I, in a recent paper Arenzon and Lemke showed for the ultradiluted Hopfield model (without refractory period) that the analytical approach is

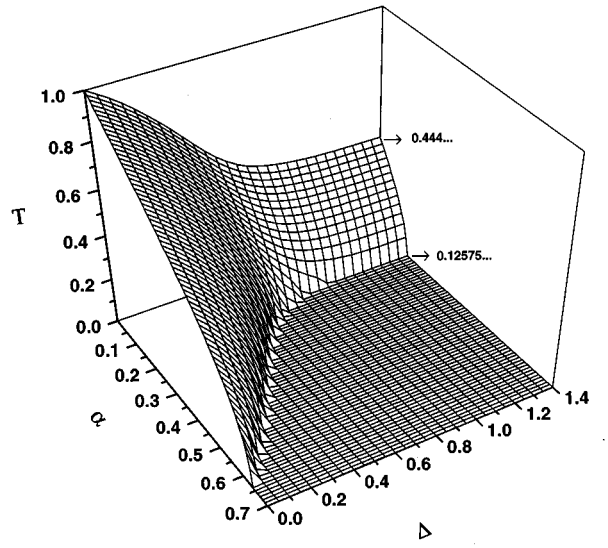

FIG. 5. Critical surface separating the retrieval phase (below) from the nonretrieval phase (above) in the space of parameters (T,α,Δ).

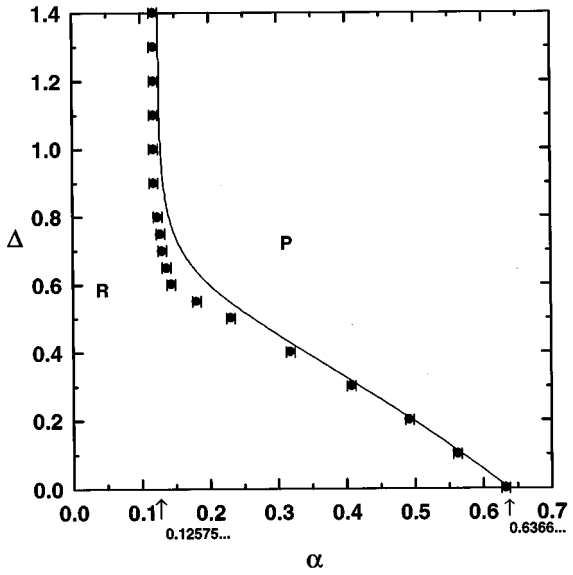

FIG. 6. The critical line separating the paramagnetic and retrieval phases in the Δ vs α plane at $T=0$. The solid line corresponds to the analytical solution for $l\to\infty$. The full circles correspond to the numerical simulations with $C=80$ and $N=80\,000$.

also valid for the less strong condition $C\ll N$. To implement the evolution of the system we use a synchronous updating dynamics, which can be conveniently expressed in terms of the overlap between the states $\{S_i\}$ and the first memory ξ_i^1 (7) as follows:

$$S_i(t+1)=\mathrm{sgn}\left[\xi_i^1 m(t)+\frac{1}{C}\sum_{q=1}^{C}\sum_{\mu\neq 1}^{p}\xi_i^\mu\xi_q^\mu S_q(t)-\frac{\Delta}{2}(S_i(t)+1)\right]. \tag{20}$$

Here the first term (signal) tends to align the system with the stored pattern, the second one acts as a noise due to all the other uncorrelated patterns, and the last one models the effect of the refractory periods.

To analyze the recognition ability we always start with an initial configuration correlated with the first memory. After an initial transient, we measure the temporal average of the overlap $m(t)$ between the first pattern and the state of the system. This procedure is repeated for 50 different samples using different memories, initial configurations, and random number sequences, in order to make a configurational average m. We work with systems of sizes $N=40\,000$ and 80 000, and with connectivity $C=40$ and 80.

In Fig. 6 we display the phase diagram Δ vs α for $T=0$. The full line corresponds to the analytical critical line in the $C\to\infty$ limit, and the full circle are the results of our numerical simulations for $N=80\,000$ and $C=80$. Note that, for small and large values of Δ, both results agree very well. In the first case (small Δ) the feedback effect due of the states $S=1$ is not very important compared to large signal term. In this region the Markovian process given by mean-field approximation presents similar results.

For large Δ, the whole history of the system is decisive in the behavior of the network. Since the parameter Δ is greater than the signal term, the temporal evolution drives the system to a regime where (i) all those neurons for which the first memory is in an inactive state ($\xi_i^1=-1$) align with the memory ($S_i=-1$); and (b) all those neurons for which the first memory is in an active state $\xi_i^1=1$ oscillate between the active and inactive states. Of course this behavior is destabilized by the effect of the other memories as α increases. For small α the system is characterized by a periodic regime (cycles of order 2) around of $m(t\to\infty)\simeq 0.5$.

In Figs. 7(a) and 7(b) we present the overlap as a function of α for $T=0$ along two cuts, $\Delta=0.2$ and 0.7, respectively. Observe that for $\Delta=0.2$ the analytical (full line) and the simulations (symbols) agree well. On the other hand, for $\Delta=0.7$ [Fig. 7(b)], the numerical results only describe the behavior qualitatively. In particular, note that it shows the coexisting phase. The dashed line indicates the unstable solution that separates the two basins of attraction, and which has not been studied numerically.

In Fig. 8 we plot $\|m(t)\|$ versus the time for $\Delta=1.4$, $N=80\,000$, $C=80$, and several values of α. Since we are considering a large value of Δ and $m(0)=1$, in the first Monte Carlo step the dynamics drives the system to a state with $m\approx 0$, from which it sometimes evolve to the antimemory instead of the memory. Because the system recognizes both the memory and the antimemory, we prefer to consider the modulus of the overlap. For small $\alpha=0.0375$ the final overlap converges to the cycle 2 regime with a mean value of around $m\simeq 0.3$, signaling the existence of spurious states (not predicted by the analytical approach). As α increases, the spurious states vanish, and the overlap reaches the attractor (mean value) $m\simeq 0.5$. The amplitude of the oscillation of the cycle-2 attractor diminishes with α, staying

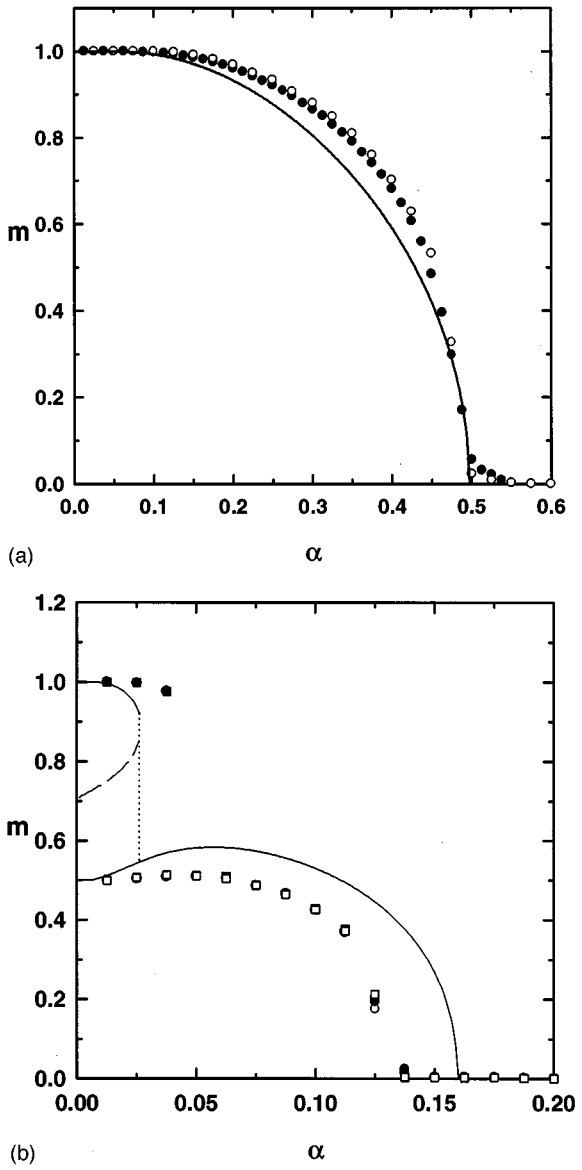

FIG. 7. The overlap m vs α at $T=0$. The full lines correspond to the analytical solutions. (a) $\Delta=0.2$ with, $m_0=1$, $N=80\,000$, $C=40$ (empty circles), and $C=80$ (full circles). (b) $\Delta=0.70$, with $C=80$: the empty circles and squares correspond to $m_0=0.6$ for $N=40\,000$ and 80 000, respectively. The full circles and squares correspond to $m_0=1$ for $N=40\,000$ and 80 000, respectively.

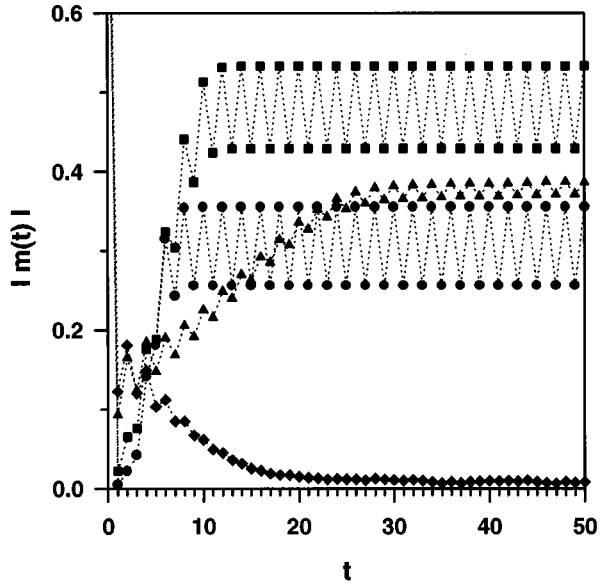

FIG. 8. $\|m(t)\|$ vs t for $C=80$, $N=80\,000$, $\Delta=1.4$, and $\alpha=0.0375$ (full circles), 0.05 (full squares), 0.1 (full triangles), and 0.125 (full diamonds).

near its mean value. For large α, the attractor converges to a regime with cycle of order greater than 2 or chaotic orbits (not the retrieval phase).

V. CONCLUSIONS

In this paper we analyze the dynamics of a neural network with random dilution and asymmetry in the synaptic couplings, and also included a threshold that mimics the refractory periods. This last ingredient is introduced through a time dependent threshold that gives place to feedback effects on the dynamics of the system. We introduce and develop an analytical method that allows us to study the long-time behavior of the system. By neglecting temporal correlations we were able to take into account the whole history of the system, and so analyze how the refractory periods affects the dynamics and the retrieval ability of our model.

We obtain the complete phase diagram of the model both analytically and numerically. Unlike the fully connected Hopfield model with refractory periods [19], for which a large value of Δ destabilizes the stored patterns completely, in the strongly diluted version we verify that for small values of α the system can *always* retrieve the pattern, irrespective of the value of Δ. Actually, for large Δ the retrieval is performed through periodic orbits (cycle 2) whose mean overlap is well predicted by the fixed point assumption. For intermediate values of Δ and small values of α, an unexpected recognition phase appears where the network can retrieve the pattern with high or low quality, depending on how far from the patterns one starts. In this region, both the effect of the Hopfield term (the signal) and the effect of the refractory period compete, given place to these two different solutions.

Our analytical results agree very well with those obtained by numerical simulations for small and large values of Δ. In the intermediate region $0.5<\Delta<1.0$, where our approach seems to be not very good (because temporal correlations are important), it predicts qualitatively well the observed results.

ACKNOWLEDGMENTS

We thank the Núcleo de Computação de Alto Desempenho (NACAD) da Coordenação de Projetos e Pesquisa em Engenharia (COPPE-UFRJ) for use of the Cray. This work was supported by Brazilian agencies CNPq, CAPES, and FINEP, and the Argentinean agencies CONICOR and SECyT (UNC).

[1] J. J. Hopfield, Proc. Natl. Acad. Sci. USA **79**, 91 (1992).
[2] D. J. Amit, H. Gutfreund, and H. Sompolinsky, Phys. Rev. A **32**, 1007 (1985); Ann. Phys. **173**, 30 (1987).
[3] A. C. C. Coolen and D. Sherrington, Phys. Rev. Lett. **71**, 3886 (1993).
[4] A. C. C. Coolen and S. Franz, J. Phys. A **27**, 6947 (1994).
[5] H. Gutfreund and M. Mezard, Phys. Rev. Lett. **61**, 235 (1988).
[6] T. L. H. Watking and D. Sherrington, Europhys. Lett. **14**, 791 (1991).
[7] H. Sampolinsky and I. Kanter, Phys. Rev. Lett. **57**, 2861 (1986).
[8] T. Fukai and M. Shiino, Phys. Rev. Lett. **64**, 1465 (1990).
[9] A. C. C. Coolen and D. Sherrington, J. Phys. A **25**, 5493 (1992).
[10] B. Derrida, E. Gardner, and A. Zippelius, Europhys. Lett. **4**, 167 (1987).
[11] J. J. Arenzon and N. Lemke, J. Phys. A **27**, 5161 (1994).
[12] J. Buchmann and K. Shulten, Biol. Cybern. **54**, 319 (1986); **56**, 313 (1987).
[13] M. Y. Choi, Phys. Rev. Lett. **61**, 2809 (1988).
[14] D. Horn and M. Usher, Phys. Rev. A **40**, 1036 (1989).
[15] K. Aihara, T. Takabe, and M. Toyoda, Phys. Lett. A **144**, 333 (1990).
[16] D. J. Amit, M. R. Evans, and M. Abeles, 1990 Network **1**, 381 (1990).
[17] W. Gerstner and J. L. van Hemmen, Network **3**, 139 (1992).
[18] F. A. Tamarit, D. A. Stariolo, S. A. Cannas, and P. Serra, Phys. Rev. E **53**, 5146 (1996).
[19] C. R. da Silva, F. A. Tamarit, and E. M. F. Curado, Int. J. Mod. Phys. C **7**, 43 (1996).